9. Absolute Ages in Resurfaced Units – Refinement of the Method

The determination of absolute ages on Mars and other solid surface objects is based on the crater production function (Ivanov, 2001, originally in Neukum (1983)) and the applied chronology model (Hartmann and Neukum, 2001). The crater production function describes the expected crater size–frequency distribution recorded in a geological unit at a specific time. This function is scaled from the well established lunar crater production function (Neukum, 1983; Neukum and Ivanov, 1994) to Mars, given the assumption that the inner solar system craters are produced by a single–source population: asteroids, ejected from the asteroid main belt between Mars and Jupiter (e.g. Neukum and Ivanov, 1994; Ivanov, 2001). The lunar crater production function could be determined over the full size range based on multi-resolution image data (which are used here; Neukum, 1983, or Hartmann (1973)). The transfer from the Moon to Mars is based on the calculation of the impacting body flux ratio between the lunar case to Mars under celestial mechanical aspects and the consideration that the condition of the crater formation differ from one planet to another, mainly in gravity and target properties of the impacted body. The validity of this approach has been demonstrated by Neukum and Wise (1976) (and later by Neukum and Ivanov (1994)) by comparing measured crater size–frequency distributions of Mars and the Moon.

To estimate the absolute age of the surface, a chronology model must be applied. This chronology model is based on measurements of the crater size–frequency distribution on areas of the Moon which could be linked to radiometric ages retrieved from sample return missions of lunar rocks (see Chapter 4). This distribution is transferable to other planets and solid surface bodies, assuming that all bodies have suffered from the heavy bombardment period that is generally reflected in the crater frequency, and in the basin population on both bodies (e.g. Neukum and Wise, 1976; Neukum and Hiller, 1981; Hartmann, 1973, 1977, 1978, and unified in Hartmann and Neukum (2001)). The idea of a marker horizon (Wetherill, 1975) specifies that large impact basins on any planet did not form any later than about 3.8–3.9 billion years ago (see Section 13).

Previously, it was almost impossible to determine and verify the predicted crater size–frequency distribution on Mars due to the fact that the image data (in terms of image resolution and covered area) did not reveal craters over the full size–range. During the Viking mission, global coverage was aquired at an average image resolution of about 231m/pxl (Viking MDIM2.1), and allowed confident investigation of the crater distribution larger than about 2 km. For selected areas medium–resolution imagery (about 70 m/pxl) and high-resolution mosaics (about 15m/pxl) exist. During the Mars Global Surveyor mission, the high–resolution Mars Orbiter Camera (MOC, 3-6m/pxl) covered many spots on the Martian surface and revealed very recent geological activity. It is difficult to link the high–resolution MOC imagery to low–resolution Viking imagery (see Chapter 12). Currently, the thermal emission imaging system (THEMIS, 18 m/pxl) onboard Mars Odyssey and the high–resolution stereo camera (HRSC, 12m/pxl) onboard Mars Express are scanning the Martian surface and provide the opportunity to fill the resoluion gap, and to define the full crater size–frequency distribution.

The procedure for determining absolute surface ages by counting craters is illustrated in Fig. 9.1. First, geological units are mapped and their area (in km^2) is determined. Following morphologic or spectral information, different units are delinated, accordingly. Here, the Mars Express–HRSC digital image obtained during

orbit 1087 is used as an example. It shows part of the caldera of Meroe Patera, a volcano in the center of the Syrtis Major volcanic province.

Crater counts are carried out by measureing the diameters with high precision. A traditional photogrammetric instrument, a Zeiss PS2K stereocomparater, was used to measure photo coordinates on transparencies. Therefore, the digital and mapped image was exposed to large–size photographic film (20 x 24 cm). The crater rim diameters were measured in microns (μm), and the maximum error in locating the stereocomparator cursor on a crater rim is on the order of 5 microns. Each measured diameter is converted into kilometers using a calibration factor depending on the pixel resolution of the digital image. The measured craters are sorted according to the quasi–logarithmical scheme described in Chapter 8. Graphically, they are represented in a cumulative crater size–frequency distribution diagram (plotted in double–logarithmic scale). The cumulative crater frequency N_{cum} is the number of craters greater than or equal to a crater diameter D_{ref} per normalized unit area (in km^{-2}). Therefore, the crater frequency reflects relative ages between various geological units. Based on fitting the crater production function (Chapter 4) to the measured crater distribution of a given geological unit by a nonlinear regression (least square), a crater retention (or relative) age is calculated directly from the fitted curve.

Two phenomena, saturation or geological resurfacing, cause characteristic deviations from the crater production function. In densely cratered units ($\hat{=}$ old), crater destruction and production eventually reach a steady state, starting at small sizes. Such an equilibrium distribution exhibits a characteristic cumulative slope of "minus–two". Here, a drop in the distribution is observed due to resurfacing of the caldera floor, hence the crater production function fits only part of the measurement and yield two ages (for details see Chapter 9.1).

Relative crater retention ages obtained by applying the cratering chronology model ((Hartmann and Neukum, 2001) and see Chapter 5) can be translated numerically into absolute cratering model ages (given in giga–years [Ga], 1 Ga = 10^9 years).

9.1. How Do Crater Counts Reveal Resurfacing?

Qualitatively, detailed morphologic studies of planetary surfaces yield insights into surface modification processes. Accordingly, geologic unit delineation, following morphologic or spectral characteristics, is based on superposition principles and other stratigraphic relations between different surface units. Quantitatively, the relative abundances and size distributions of impact craters distinguish geologic units chiefly by relative age. A combination of both facets helps to outline homogeneous geologic units. In general, remote–sensing age–dating techniques rely on imaging of planetary surfaces at high enough spatial resolution to allow adequate statistics to be developed on craters over a wide size range. For detailed crater size–frequency distribution studies, any deviation from the crater production function (see Chapter 4) implies a resurfacing event (erosion or deposition). Although a careful separation of the different units might sometimes not be possible due to image resolution, the effect of resurfacing is detectable in the crater size–frequency distribution and resurfacing ages can still be determined. Usually, resurfacing erases the cratering record starting at the smaller size range or resets the cratering record totally when the surface is completely renewed. Thus, it is dependent on the magnitude of the event. When measuring the crater size–frequency distribution of such a unit, any distinct drop in the distribution reveals a resurfacing event. In cases of ongoing resurfacing (e. g. on steep slopes of martian surface structures) or saturation, the crater counts cannot be linked to an age.

For units, where resurfacing has been observed, the determination of ages has to be limited to a certain diameter range (below or above a diameter $d_\star$, where the resurfacing has influ-

enced the crater size–frequency distribution). The oldest age is derived straightforwardly, by fitting the production function to the large–diameter range. For the resurfacing event, if no correction has been applied, the age is slightly overestimated (depending on the magnitude of the resurfacing event) due to the cumulative character of the crater size–frequency distribution. As a first attempt, a cut–off limit (Neukum and Hiller, 1981) applied to the large size range reduces the number of craters in the smaller size range, which is used to estimate the resurfacing event. This approach underestimates the age (depending on the surface age difference). For this work a more precise treatment is developed.

The general description of the cumulative crater size–frequency distribution $N_{cum}\,(D,t)$ is given by the cumulative number of craters per area for a given diameter D at a certain time t:

$$N_{cum}\,(D,\,t) = \int_{D}^{\infty}\int_{0}^{t} g\,(D')\,dD' \cdot f\,(t')\,dt' \qquad (9.1)$$

for an undisturbed geological unit a simple solution can be found:

$$N_{cum}\,(D,\,t) = G\,(D)\;\cdot\;F\,(t), \qquad (9.2)$$

where G represents the cumulative crater size–frequency distribution and F the flux of projectiles. It has been demonstrated that the crater size–frequency distribution is stable over time, but the flux decays (see Chapter 8).

In a unit where subsequent processes (erosion as well as deposition) occurred, the smaller crater population has been modified preferentially. Therefore, the measured crater size–frequency distribution will deviate from the crater–production function for craters smaller than a certain diameter $d_\star$. If the resurfacing event ended at a certain time $t_\star$, the surface accumulates craters as it is a fresh surface. In the cumulative description, the crater size–frequency distribution is represented by the sum of two (or more) populations, where the older one(s) do not cover the entire measurable size range. Such a distribution is represented by:

$$\begin{aligned} N_{eros} \;&=\; \int_{D_{min}}^{D_{max}} g\,(D')\,dD' \cdot \int_{0}^{t_\star} f\,(t')\,dt' \\ &+\; \int_{d_\star}^{D_{max}} g\,(D')\,dD' \cdot \int_{t_\star}^{t_{max}} f\,(t')\,dt', \end{aligned} \qquad (9.3)$$

where the measurement is performed with a diameter range between $D_{min} \le d_\star \le D_{max}$ and the original surface has been formed at a time t_{max}, the resurfacing ended at a time $t_\star$, with $0 \le t_\star < t_{max}$. If $t_\star = t_{max}$, no resurfacing occurred and the description follows equation 9.1 and 9.2.

On a planetary surface, a proper remote–sensing method to distinguish both populations is not known. Any attempts to distinguish between erosional state or other parameters are strongly misleading (and subjective). To understand the crater population accumulated on the surface after the resurfacing event, a method is needed to separate both populations. Due to the crater accumulation per time and the cumulative characteristics of the measured crater size–frequency distribution, the contribution of the old crater population has to be calculated with respect to their quantity in the diameter range larger than $d_\star$. The measured crater frequencies in the smaller crater size range, attributed to the resurfacing event, have to be reduced (by the number of craters produced in the period prior to the resurfacing event).

Based on the known crater–production function (see Chapter 4), the cut–off diameter and the age of the old surface can be determined, while the exact resurfacing age remains obscured:

$$\begin{aligned} N_{eros} \;&=\; \int_{d_\star}^{D_{max}} g\,(D')\,dD' \cdot \int_{0}^{t_{max}} f\,(t')\,dt' \\ &-\; \int_{d_\star}^{D_{max}} g\,(D')\,dD' \cdot \int_{0}^{t_\star} f\,(t')\,dt' \end{aligned}$$

$$
\begin{aligned}
&+ \int_{D_{min}}^{D_{max}} g\,(D')\,dD' \cdot \int_{0}^{t_\star} f\,(t')\,dt' \\
&= ((G\,(D_{max}) - G\,(D_\star)) \cdot F\,(t_{max})) \\
&- ((G\,(D_{max}) - G\,(D_\star)) \cdot F\,(t_\star)) \\
&+ ((G(D_{max}) - G(D_{min})) \cdot F\,(t_\star)) \qquad (9.4)
\end{aligned}
$$

Following the description in equation 9.3 and 9.4, a fit of the crater production function G(D) allows one to predict the shape of the expected distribution in the large–size range of the "resurfacing population", which gives a preliminary but overestimated age $t_{\star_{prelim}}$. Next, the expected number of craters accumulated on the younger surface is predicted. Thus, the contribution (in number) of the old crater population in the large branch can be calculated and the measured number of craters at the cut–off diameter $d_\star$ reduced, accordingly. By fitting the reduced distribution, the younger age is correctly determined.

Equation 9.4 demonstrates that an iterative approach is necessary to determine the age(s) of resurfacing event(s) by fitting the well known crater production function to the crater size range smaller than a certain diameter $d_\star$ and to predict the expected number of craters for diameters larger than diameter $d_\star$. Reducing the measured number to the predicted one allows for the determination of the time when the resurfacing event ended, and therefore, the age of the younger surface. The proper treatment of the cumulative crater numbers, which reduces the influence of the large–crater range on the age determination for the subsequent events, is illustrated in Figure 9.1: First, the crater production function is fitted to the measured crater size–frequency distribution in the appropriate size ranges (below and above $d_\star$). The fit for the large size range is straightforward for the old surface (above $d_\star$). The fit to the crater range (below $d_\star$) representing the subsequent event is used to calculate the expected contribution of craters on a surface of that age. The excess in the large–size range is now easily determined and the measured crater size–frequency distribution can be corrected by the difference of the measured and the expected number of craters at the cut–off diameter. Finally, the corrected cumulative crater size–frequency distribution can be used to derive the resurfacing age. In cases where additional resurfacing processes took place, the correction has to be repeated at the next cut–off diameter.

A typical example of a crater size–frequency distribution is that for the Meroe Patera caldera in the Syrtis Major volcanic province (Fig. 9.1). Resurfacing has occurred and is clearly visible in Figure 9.1, B. The age has been determined at 3.73 Ga and resurfacing at 3.08 Ga. Fig. 9.1 (C) shows the effect on the younger age if a cut–off limit has been used to clear the cumulative crater number in the smaller size range (following Neukum and Hiller, 1981). The calculated age is 1.88 Ga, i.e. much younger. Fig. 9.1 (D) shows the results of treating the crater size–frequency distribution with the previously explained approach. This shows a more accurate 2.33 Ga age for the resurfaced surface. The age differences ($t_{cut-off} \leq t_\star \leq t_{\star_{prelim}}$) between these three approaches of determining the resurfacing event at a time $t_\star$ depend on the magnitude of the event and the time difference between the original surface formation and the modification event. Resurfacing ages described subsequently follow the approach developed here.

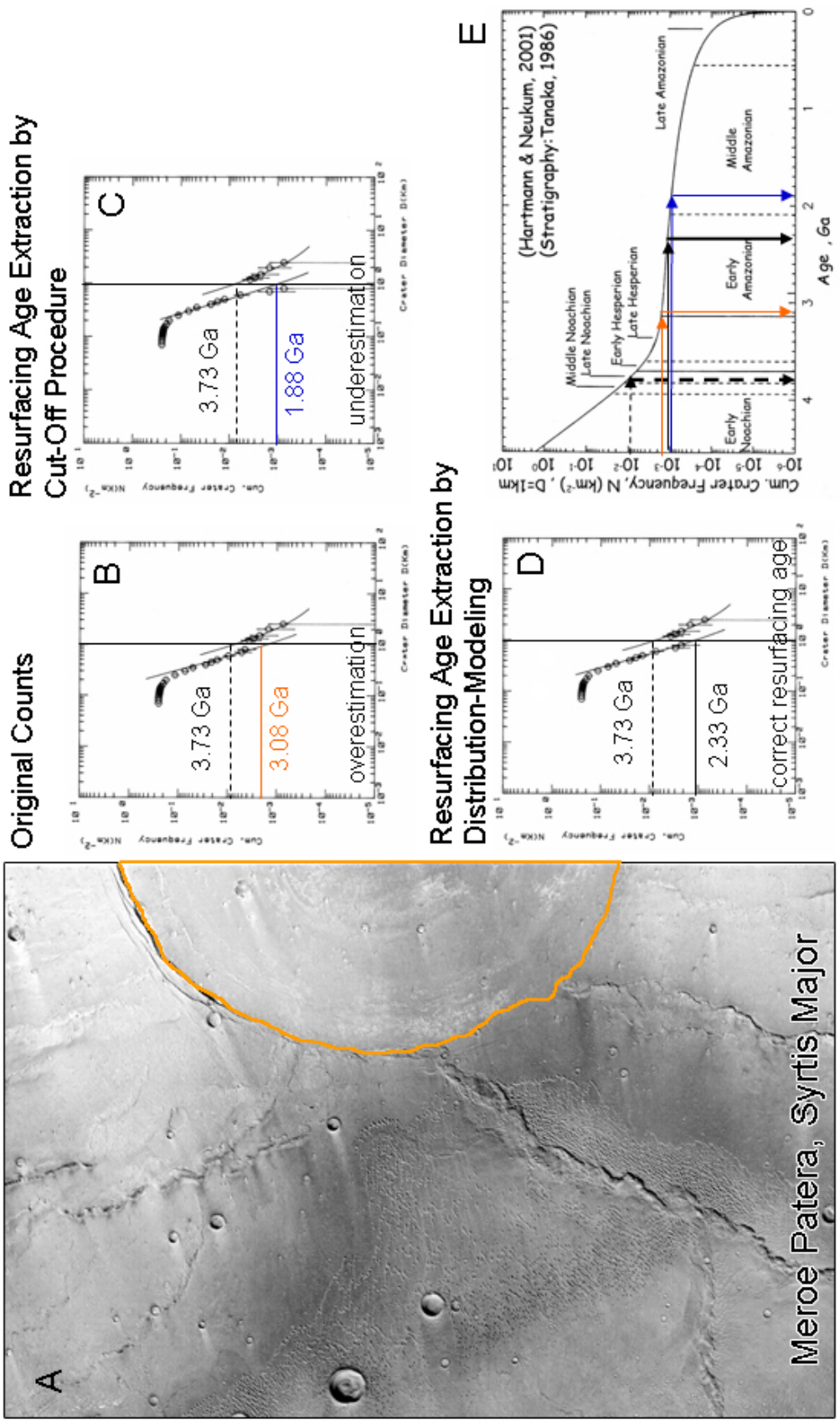

Figure 9.1.: Example of Age Determination of the Meroe Patera Caldera (Syrtis Major volcanic province)

Figure 9.1.: (Cont.) Example of Age Determination of the Meroe Patera Caldera (Syrtis Major volcanic province) and Age Extraction When Resurfacing Occurs: (A) A geological unit is delinated according to the caldera morphology. (B, C, D) Crater counts have been performed, and plotted as cumulative frequency versus diameter (in double–logarithmic scale). The crater–production function was fitted to the measured distribution, yielding at least one resurfacing event. The fitted polynomial is a measure of the relative age of the surface. The area and thus the crater size-frequency distribution observed was affected by resurfacing processes at some time in its geologic history. Therefore, the crater frequency (kink) drops, and deviates from the calibration distribution below a certain crater diameter. To extract the time of the resurfacing event (the age of the resurfaced area) the small and large crater branches can be separated as shown in this diagram. (B) shows the originally measured distribution, (C) the result if all craters larger than a certain diameter (cut-off diameter) are removed, and (D) shows the result if only part of the underlying distribution is removed. The curves are fitted to certain size ranges. The resulting age for the end of the resurfacing period differs according to the approach. (E) The cumulative number of craters for N (D = 1 km) is transfered to an absolute surface age by applying the Martian cratering chronology model (Hartmann and Neukum, 2001). The age determined indicated by the black lines (solid and dashed) are the best estimate, because for the resurfacing event the large craters are included in the right proportion (D).